Proceedings of IDETC/CIE 2007
ASME 2007 International Design Engineering Technical Conferences & Computers and Information in Engineering Conference
September 4-7, 2007, Las Vegas, Nevada, USA

DRAFT: DETC-35295

HLPR CHAIR: A NOVEL INDOOR MOBILITY-ASSIST AND LIFT SYSTEM

Roger Bostelman, James Albus, Tommy Chang, Tsai Hong
Intelligent Systems Division
National Institute of Standards and Technology (NIST)
Gaithersburg, MD 20899
301-975-3426, roger.bostelman@nist.gov

Sunil K. Agrawal, Ji-Chul Ryu
Mechanical Systems Laboratory
Department of Mechanical Engineering
University of Delaware, Newark, Delaware 19716
Email: agrawal,jcryu@udel.edu

ABSTRACT
This paper describes a novel Home Lift, Position, and Rehabilitation (HLPR) Chair, designed at National Institute of Standards and Technology (NIST), to provide independent patient mobility for indoor tasks, such as moving to and placing a person on a toilet or bed, and lift assistance for tasks, such as accessing kitchen or other tall shelves. These functionalities are currently out of reach of most wheelchair users. One of the design motivations of the HLPR Chair is to reduce back injury, typically, an important issue in the care of this group. The HLPR Chair is currently being extended to be an autonomous mobility device to assist cognition by route and trajectory planning. This paper describes the design of HLPR Chair, its control architecture, and algorithms for autonomous planning and control using its unique kinematics.

1 INTRODUCTION
'Today, approximately 10% of world's population is over 60, by 2050 this proportion will have more than doubled' and 'the greatest rate of increase will be amongst the oldest, people aged 85 and older' [1]. This elderly group is subject to both physical and cognitive impairments, more than younger people. These will have a profound impact on how we will maintain independence of the elderly from caregivers. For decades, assistive technology for the mobility impaired has included wheelchairs, lift aids and other devices. However, a subject in a wheelchair typically needs assistance from others for navigation in cluttered areas or in transfers to a bed or a toilet. With potentially more elderly users, there is a need to improve these mobility devices so as to reduce dependence on others.

1.1 Wheelchairs
There has been an increasing need for wheelchairs over time. 'Mobility is fundamental to health, social integration and individual well-being of the humans. Henceforth, mobility must be viewed as being essential to the outcome of the rehabilitation process of wheelchair dependent persons and to their successful (re-)integration into society and to a productive and active life' [2]. Many lower limb disabled subjects depend upon a wheelchair for their mobility. 'Estimated numbers for Europe and USA are respectively 2.5 million and 1.25 million. The quality of the wheelchair, the individual work capacity, the functionality of the wheelchair/user combination, and the effectiveness of the rehabilitation program do indeed determine the freedom of mobility' [3].

1.2 Patient Lift
There is a great need for lift devices to transfer patients into wheelchairs, beds, automobiles, etc. The need for lift devices will also increase as the generation gets older. Here are some important remarks to consider - 'The question is, what does it cost not to buy this equipment? A back injury can cost as much as $50,000, and that is not even including all the indirect costs. If a nursing home can buy these lifting devices for $1,000 to $2,000, and eliminate a back injury that costs tens of thousands of dollars, thats a good deal' [4]. 'One in every three nurses be-

comes injured from the physical exertion put forth while moving non-ambulatory patients, costing their employers $35,000 per injured nurse' [5]. 'One in two non-ambulatory patients falls to the floor and become injured when being transferred from a bed to a wheelchair' [6]. 'Nursing and personal care industry ranks among the highest in terms of injuries and illnesses, with rates about 2.5 times that of all other general industries' [7]. 'In 1950, there were 8 adults available to support each elder 65 and over, today the ratio is 5 to 1 and by 2020 the ratio will drop to 3 working age adults per elder person' [8].

Motivated from these findings, NIST surveyed technology for patient lift and mobility devices [9]. The report showed that there is need for intelligent wheelchair technology that integrates mobility with lift to maneuver patients and also rehabilitate them to gain more independence. Even though many research efforts have been reported on intelligent wheelchairs, e.g. [11, 12, 13, 14], the authors have seen a lack of standard control methods or the use of advanced 3D imagers on intelligent wheelchairs [10]. These issues have motivated NIST to develop the HLPR Chair. This paper describes its novel mechanical design features, its system architecture, and algorithms for planning and control using its intrinsic kinematics.

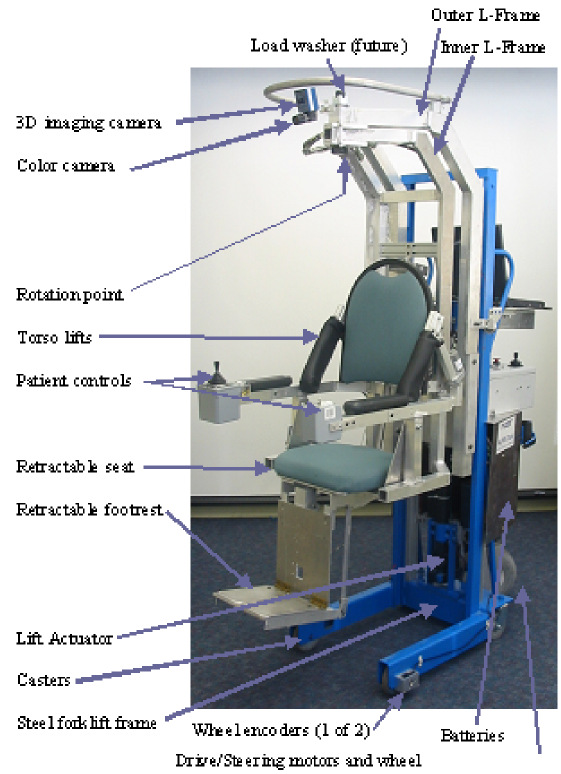

Figure 1. Photograph of the HLPR Chair prototype.

2 HLPR Chair Structure and Design

The HLPR Chair prototype, shown in Figure 1, is based on a manual, off-the-shelf, sturdy forklift. The forklift includes a U-frame base with casters in the front and rear and a rectangular vertical frame. The lift and chair frame is 58 cm wide, 109 cm long, and 193 cm high, making it small enough to pass through most residential bathroom doors. The patient sit-stand mechanism includes an outer frame that extends an upper rotation point above the front caster wheels. The inner frame, which supports the seat and footrest assemblies, rotates about the outer frame pivot point placing the patient outside the HLPR Chair wheelbase. The L-shaped frames are made of square, aluminum tubing welded as shown in the photograph. The outer L is bolted to the lift device while the inner L rotates with respect to the seat base frame at the end of the L as shown in Figure 1. The frame's rotation point is above the casters at the very front of the HLPR Chair frame to allow for outside wheelbase access when the seat is rotated by 180 deg.

Drive and steering motors, batteries and control electronics along with their aluminum support frame provide counterweight for the patient to rotate beyond the wheelbase. When not rotated, the center of gravity remains near the middle of the HLPR Chair. When rotated to 1 rad (180 deg) with a 136 kg (300 lbs) patient on board, the center of gravity remains within the wheelbase for safe seat access. Heavier patients would require additional counterweight.

The HLPR Chair has a tricycle design to simplify the steering and drive linkages and provide a compact drive system. The drive motor is mounted perpendicular to the floor and above the drive wheel with chain a drive. The steering motor is coupled to an end cap on the drive motor and provides approximately 180 deg rotation of the drive wheel to steer the HLPR Chair. The front of the robot has two casters mounted to a U-shaped frame. The prototype motors are 1/2 hp for drive and 1/17 hp for steering. The drive motor is geared such that its high speed drives a chain driven wheel providing further speed reduction. HLPR Chair speed is 0.7 m/s. While this is sufficient speed for typical eldercare needs, a more powerful motor can replace the drive motor for additional speed.

Steering is a novel single wheel design with a hard stop beyond ± 90 deg for safety of the steering system. Steering is reverse Ackerman controlled by a joystick, left rotates the drive wheel counterclockwise, and right clockwise. For access to the HLPR Chair and for mobility, the HLPR Chair is lowered. A seat belt or harness is required for occupant safety. For access/exit to/from the HLPR Chair, the footrest can be retracted beneath the seat. For mobility, the footrest is deployed to carry the feet. Also, manually rotated feet pads can be deployed to provide a wider footrest. When retracted, the footrest pads automatically rotate within the footrest volume.

Patient lift is designed into the HLPR Chair to allow user access to high shelves or other tall objects while seated. The HLPR Chair's patient lift is approximately 1 m to match the reach of a tall person. This is a distinct advantage over marketed chairs and other concepts [15]. The additional height comes at no additional cost of frame and only minimally in actuator cost. Lift is achieved by a 227 kg (500 lbs) max lift actuator that can support 681 kg (1500 lbs) on the HLPR Chair. The actuator connects to a lift plate with a steel chain that is mounted at one end to the HLPR Chair frame and to the lift plate at the other end. The actuator pushes up on a sprocket providing approximately 1 m (36 inches) lift with only a 0.5 m (18 inches) actuator stroke. The outer L-frame is bolted to the lift plate. Rollers mounted to the lift plate roll inside the HLPR Chair vertical C-channel frame. HLPR Chair rehabilitation configuration is also explained in [15]. In this configuration, HLPR Chair will potentially allow, for example, stroke patients to keep their legs active without supporting the entire load of the patients body weight. This is similar to body weight support system often used in BWSTT, a pardigm currently useful for treadmill training of spinal cord injury patients [16]. The patient, once lifted, could walk while supported by the HLPR Chair driving at a slow walking pace towards regaining leg control and eliminating the need for a wheelchair.

2.1 Seat Placement Using HLPR Chair

It is estimated that 1 in 3 nurses or caregivers develop back injuries while attending to patients[9]. These injuries occur because the patient is relatively heavy to lift and access to the patient is difficult when attempting to place in another seat. Additionally, wheelchair dependents have difficulty moving to or from a seat without a caregiver's help or other lift mechanisms. The HLPR Chair has been designed for patient lift, as explained previously, not only to access tall objects but also to pick and place the patient in other chairs, toilets, or beds. Figure 2(i) shows the concept of placing a patient on another seat, such as a toilet.

To place a HLPR Chair user on another seat, the user first drives to the seat. Once there, the HLPR Chair rotates the footrest up and beneath the seat and the patient's feet are placed on the floor. The HLPR Chair inner L-frame can then be rotated manually with respect to the chair frame allowing the patient to be above the toilet. Padded torso lifts the patient from beneath his/her arm joints similar to crutches. The seat, with the footrest beneath, then rotates from horizontal to vertical behind the patients back clearing the area beneath the patient to be placed on the toilet. Once the person is placed on a toilet, the HLPR Chair can remain in the same position to continue supporting them from potential side, back or front. However, when placing a person onto a chair, the HLPR Chair must lift the patient and the patient manually rotates the chair from around the patient and out of the patients space. Figure 2(ii) shows the HLPR chair in these configurations.

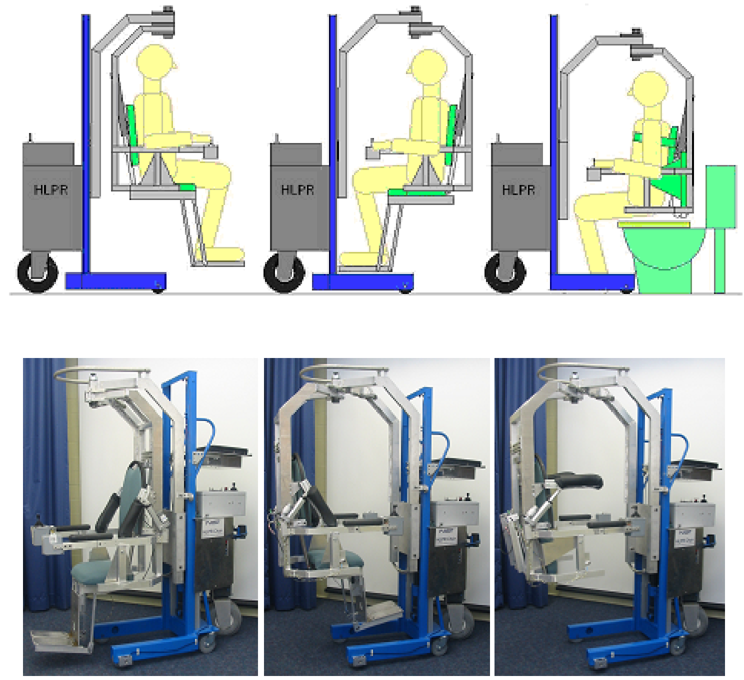

Figure 2. (i) Graphic showing the concept of placing a patient onto a toilet or chair with the HLPR Chair. The patient drives to the target seat (left), manually rotates near or over the seat (middle) and then while the torso lifts support the patient and the seat retracts, the patients is then lowered onto the seat - toilet, chair or bed (right); (ii) Photographs of the HLPR Chair in the same configurations as in the left, center, and right graphics, respectively, showing patient placement onto another seat.

3 System and Control Architecture for HLPR Chair

The HLPR Chair controls include a joystick for drive and steering control and a rocker switch for lift control. There are also switches to control seat and footrest retraction or deployment. Behind the seat and frame and above the drive/steer wheel is the electronics box that houses the control relays for the HLPR Chair while also providing a 'Nurse' or caregiver control panel that duplicates the patient controls at the seat. The Nurse control panel includes all the control functions for a nurse or caregiver to drive or lift a patient. Control redundancy is designed into the HLPR Chair to provide dependent mobility and lift for dependent patients. A 'Nurse/Patient' switch also included on the Nurse control panel allows switching between the rear (Nurse) control and the chair (Patient) control.

To get patients into a bathroom or maneuver through tight spaces, the HLPR Chair operator is required to have sufficient skill to drive to the toilet through small doorways and to dock with the toilet. Although the HLPR Chair is narrow enough to fit through relatively small doorways, it would be difficult for even skilled operators to navigate through the doorway without bumping into the doorframe and causing damage. Hence, there is a need to develop autonomous navigation algorithms.

Recently, the HLPR Chair was modified to include encoders, attached between it's frame and front caster wheels, and a computer interface. Although the encoder and housing add an additional 2.5 cm to each side of the base, the overall HLPR Chair base width is still within the chair-frame width and therefore, within the overall HLPR Chair width of 58 cm. The encoders provide approximately 90 pulses/cm of linear travel. The relatively high measurement accuracy of the wheels will help develop accurate path planning and control algorithms for the HLPR Chair.

Included in the 'Nurse' control panel is a switch to toggle between computer and manual modes. During computer control, drive and steer are controlled by an onboard computer laptop with off-the-shelf input/output (I/O) devices housed in the box beneath the PC and connected through a universal serial bus (USB) interface. This design was chosen as a simple developer interface to the HLPR Chair prototype knowing that the computer and it's interfaces can be significantly reduced in size as future commercial versions are designed. Software drivers for the HLPR Chair drive and steer control were written in C++ under the Linux operating system. NIST standard software control architecture for intelligent machines '4D/RCS (4 dimensional/ Real-time Control System)' integrated with robot's behavior generation [16]. The autonomous control will be based on sensing of the environment around the robot to localize it within a world model. Appropriate navigational trajectories and motor torque inputs will be determined in near real time. The HLPR Chair plans to adopt the 4D/RCS control architecture so that advanced 3D imagers and control algorithms can be plug-and-played to address the variety of patient mobility controls that may be needed.

4 Planner and Controller for HLPR Chair Using Differential Flatness

Most wheelchairs are differentially driven through their wheels, i.e., if the right wheel is spun faster than the left wheel, the vehicle moves towards the left and if both wheels spin at the same rate, the vehicle travels straight. This is also the principle for manual drive of wheelchairs. However, due to its unique design, the vehicle is driven and steered through its rear wheel. This allows the motors and drive electronics to be placed behind the user and makes it compact and safe.

In this section, we describe a method for trajectory planning and control of HLPR Chair which exploits its non-holonomic constraints, resulting from no-slip constraints of the wheels, to show that this system is differentially flat. With this property, the system is both controllable and diffeomorphic to a chain of integrators through dynamic feedback linearization [17]. The resulting chain of integrator form is then used to efficiently plan and control the motion of the vehicle. Even though the methods of differential flatness are gaining prominence in design, trajectory planning, and control of a wide variety of dynamic systems including mobile robots, micro air vehicles, the use of these algorithms within the the next generation mobility assist machines is novel and allows to create near real-time implementations [18-22].

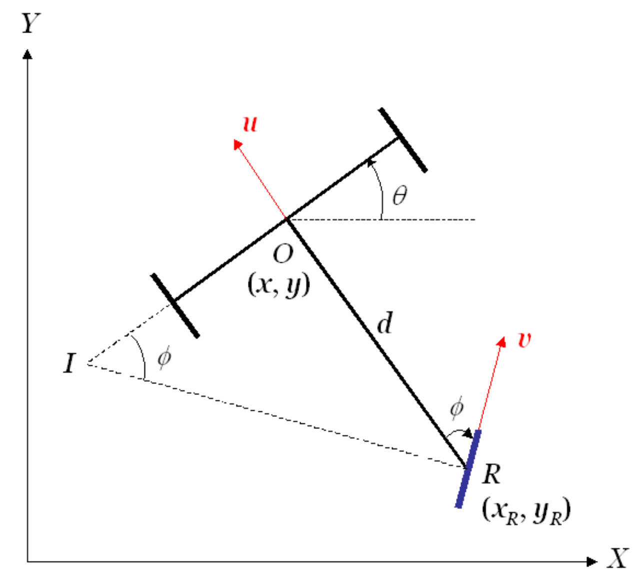

Figure 3. The real wheel-drive of HLPR chair in Cartesian space described by (x, y, θ, ϕ).

A schematic of the HLPR chair is shown in Fig. 3, where the rear wheel is both driven and steered. The inputs to this system are the driving speed v and the steering angle of the rear wheel ϕ. As described in other referenes of the authors, it is also possible to develop planners and controllers for this vehicle which take into account the full dynamics of the vehicle, as opposed to only the kinematic model. The inputs to this dynamic model would be the motor torque inputs at the rear wheel. However, due to space limitations, the dynamic model and trajectory planning and control methods using this dynamic model are not included in this paper.

4.1 Kinematics of HLPR

In Cartesian coordinates, the system's configuration is given by

$$\mathbf{q} = [x, y, \theta, \phi]^T, \qquad (1)$$

where x, y are the position of the midpoint O of the front wheel axle. θ is the angle of the frame and ϕ is the heading angle of the driving wheel with respect to the frame. d is the length from the center of the driving wheel to the midpoint of the front wheel axle. Fig. 3 shows the schematic of the system and its configuration. From the geometric relationship, the center position R of the driving wheel is given as $x_R = x + d\sin\theta, y_R = y - d\cos\theta$.

From the assumption of no-slip on the wheels, one gets nonholonomic constraints of the form

$$C(\mathbf{q})\dot{\mathbf{q}} = 0, \tag{2}$$

where

$$C(\mathbf{q}) = \begin{pmatrix} \cos(\phi-\theta) & -\sin(\phi-\theta) & d\cos\phi & 0 \\ \cos\theta & \sin\theta & 0 & 0 \end{pmatrix}. \tag{3}$$

With a matrix $S(\mathbf{q})$ that spans the null space of $C(\mathbf{q})$, it is possible to define the velocity vector $\nu(t)$ such that

$$\dot{\mathbf{q}} = S(\mathbf{q})\nu(t). \tag{4}$$

Hence, if we represent the velocity vector ν as the heading speed v and the turning speed $\dot{\phi}$ of the driving wheel, or $\nu = [v \;\; \dot{\phi}]^T$, such a matrix $S(\mathbf{q})$ is given by

$$S(\mathbf{q}) = \begin{pmatrix} -\sin\theta\cos\phi & 0 \\ \cos\theta\cos\phi & 0 \\ \sin\phi/d & 0 \\ 0 & 1 \end{pmatrix}. \tag{5}$$

Therefore, (4) represents the kinematic model of the system.

4.2 Trajectory Planner and Controller

In this section, we show that the kinematic model of this HLPR chair is differentially flat by choosing the position of the midpoint of the front wheel's axle (x, y) as flat outputs and applying input prolongations. It can be checked that the system modeled by its kinematics, $\dot{\mathbf{q}} = S\nu$, in (4) is not linearizable by prolongation [21]. Therefore, in order to find a diffeomorphism between the state variables and the flat outputs, let us introduce an input transformation such that

$$u_1 = v\cos\phi, \tag{6a}$$

$$u_2 = \dot{\phi}, \tag{6b}$$

Then, the kinematic model of the system becomes

$$\begin{aligned} \dot{x} &= -\sin\theta u_1, \\ \dot{y} &= \cos\theta u_1, \\ \dot{\theta} &= \frac{\tan\phi}{d} u_1, \\ \dot{\phi} &= u_2. \end{aligned} \tag{7}$$

Now, we apply a second order prolongation of u_1 by considering additional states z_1 and z_2 such that $z_1 = u_1$ and $z_2 = \dot{u}_1$. Consequently, the prolonged systems is given as

$$\begin{aligned} \dot{x} &= -\sin\theta z_1, \\ \dot{y} &= \cos\theta z_1, \\ \dot{\theta} &= \frac{\tan\phi}{d} z_1, \\ \dot{\phi} &= \bar{u}_2, \\ \dot{z}_1 &= z_2, \\ \dot{z}_2 &= \bar{u}_1, \end{aligned} \tag{8}$$

where

$$\bar{u}_1 = \ddot{u}_1, \bar{u}_2 = u_2. \tag{9}$$

By choosing flat outputs $F = (F_1, F_2) = (x, y)$, all state variables and two inputs can be expressed in terms of the flat outputs and their derivatives.

$$z_1 = \sqrt{\dot{F}_1^2 + \dot{F}_2^2}, \tag{10}$$

$$\theta = \tan^{-1}\left(-\frac{\dot{F}_1}{\dot{F}_2}\right), \tag{11}$$

$$z_2 = \dot{z}_1 = \frac{\dot{F}_1\ddot{F}_1 + \dot{F}_2\ddot{F}_2}{\sqrt{\dot{F}_1^2 + \dot{F}_2^2}}, \tag{12}$$

$$\begin{aligned} \phi &= \tan^{-1}\left(\frac{d\dot{\theta}}{z_1}\right), \\ &= \tan^{-1}\left(\frac{d\frac{\dot{F}_1\ddot{F}_2 - \ddot{F}_1\dot{F}_2}{\dot{F}_1^2 + \dot{F}_2^2}}{\sqrt{\dot{F}_1^2 + \dot{F}_2^2}}\right), \end{aligned} \tag{13}$$

and the inputs $\bar{u}_1$, $\bar{u}_2$ can be computed from

$$\bar{u}_1 = \dot{z}_2 = \xi_1 \dddot{F}_1 + \xi_2 \dddot{F}_2 + \xi_3, \tag{14a}$$

$$\bar{u}_2 = \dot{\phi} = \zeta_1 \dddot{F}_1 + \zeta_2 \dddot{F}_2 + \zeta_3. \tag{14b}$$

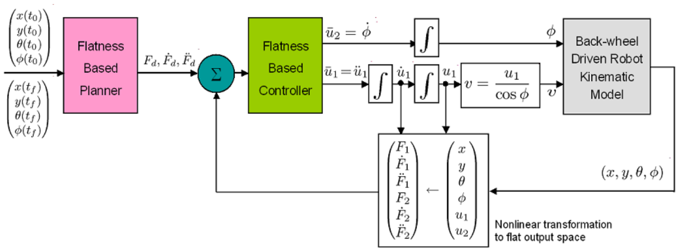

Figure 4. Integrated trajectory planning and control summary with the kinematic model of the HLPR Chair.

where ξ_i, ζ_i $(i = 1, \ldots, 3)$ are functions of $F, \dot{F}, \ddot{F}$. Hence, we are assured that F_1, F_2 are properly chosen flat outputs and the rear wheel-driven robot described by the kinematic model in (8) is a flat system.

In this framework, the initial conditions of $x(0)$, $y(0)$, $\theta(0)$, and $\phi(0)$ are used to get $F_1(0)$, $\dot{F}_1(0)$, $\ddot{F}_1(0)$, $F_2(0)$, $\dot{F}_2(0)$, and $\ddot{F}_2(0)$ with $(F_1, F_2) = (x, y)$. Similarly, $F_1(t_f)$, $\dot{F}_1(t_f)$, $\ddot{F}_1(t_f)$, $F_2(t_f)$, $\dot{F}_2(t_f)$, and $\ddot{F}_2(t_f)$ can be computed from $x(t_f)$, $y(t_f)$, $\theta(t_f)$, and $\phi(t_f)$. A smooth trajectory, which satisfies the end conditions in the flat output space, can be selected between $t = 0$ and $t = t_f$.

The prolonged kinematic system described by (8) is feedback linearizable. Hence, the system is governed by the following linearized equations.

$$\dddot{F}_1 = v_1, \dddot{F}_2 = v_2. \tag{15}$$

The feedback control laws v_1, v_2 can be chosen as

$$v_1 = \dddot{F}_{1d} + k_1(\ddot{F}_{1d} - \ddot{F}_1) + k_2(\dot{F}_{1d} - \dot{F}_1) + k_3(F_{1d} - F_1), \tag{16}$$
$$v_2 = \dddot{F}_{2d} + r_1(\ddot{F}_{2d} - \ddot{F}_2) + r_2(\dot{F}_{2d} - \dot{F}_2) + r_3(F_{2d} - F_2), \tag{17}$$

where F_{1d}, F_{2d} are desired trajectories for the flat outputs F_1, F_2, respectively and k_i, r_i $(i = 1, \ldots, 3)$ are control gains. This control law in (16) and (17) gives exponential stable error dynamics if the gains are chosen properly, i.e., make the roots of the characteristic polynomial lie in the left half plane. On substitution of (15) in (14), control inputs $\bar{u}_1$ and $\bar{u}_2$ for the prolonged system become

$$\bar{u}_1 = \xi_1 v_1 + \xi_2 v_2 + \xi_3, \tag{18a}$$
$$\bar{u}_2 = \zeta_1 v_1 + \zeta_2 v_2 + \zeta_3. \tag{18b}$$

Control inputs v, w for the original system can be calculated by going back to Eqs. (9) and (6).

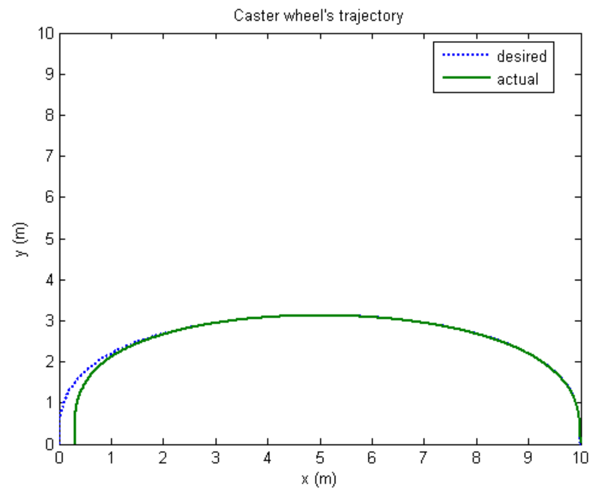

Figure 5. A sample desired and actual trajectory with the kinematics based controller. Initial error of 0.3 meter in x axis is given to check the controller performance.

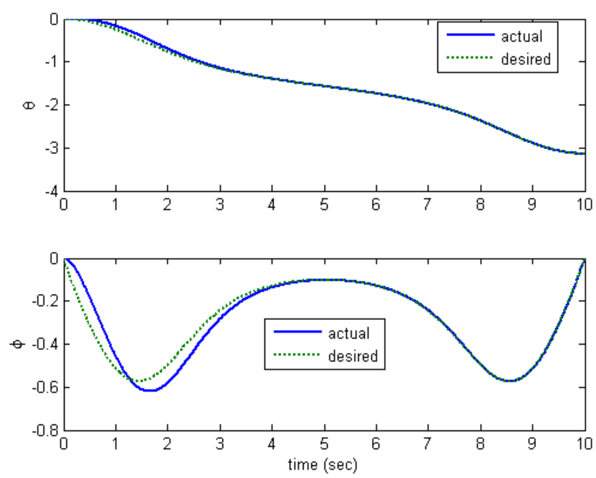

Figure 6. The angles' trajectories with the kinematic model based controller. The desired trajectory of each angle is calculated from the designed trajectories of the flat outputs F_1, F_2.

4.3 Simulation Results for point-to-point Maneuver

For illustration, fifth order polynomials are taken for the trajectories for flat outputs $F_1(t)$ and $F_2(t)$. The desired trajectories until $t_f = 10$ sec are planned with the following end conditions: $x(0) = 0$, $y(0) = 0$, $\theta(0) = 0$, $\phi(0) = 0$, $u(0) = 1$, $\dot{u}(0) = 0$, $x(10) = 10$, $y(10) = 10$, $\theta(10) = 0$, $\phi(10) = 0$, $u(10) = 1$, $\dot{u}(10) = 0$. All units are in MKS with angles in degree. Corresponding end conditions in flat output space are as follows: $F_1(0) = 0$, $\dot{F}_1(0) = 0.9848$, $\ddot{F}_1(0) = 0$, $F_2(0) = 0$, $\dot{F}_2(0) = 1$,

$\ddot{F}_2(0) = 0$, $F_1(10) = 10$, $\dot{F}_1(10) = 0$, $\ddot{F}_1(10) = 0$, $F_2(10) = 10$, $\dot{F}_2(10) = 0$, $\ddot{F}_2(10) = 0$. The structure of the integrated planner and controller which is applied to the kinematic model of the robot is shown in Fig. 4. Fig. 5 shows the planned desired trajectory and actual trajectory of the robot. In this simulation, the initial condition of $x(0)$ is taken as 0.3 being an initial error at $t = 0$. Corresponding desired trajectories and actual trajectories of θ and ϕ are shown in Fig. 6. The simulation checks the validity of the tracking controller for the kinematic model.

4.4 Simulations of a complete maneuver to a goal

An autonomous demonstration is planned to show the Autonomous mode of the HLPR Chair. It will be manually driven to a bathroom doorway at NIST and then placed in autonomous mode, with the goal to navigate through the narrow doorways and dock with the toilet. After docking, the HLPR Chair will then reverse motion and navigate back out of the room to the starting position. A graphic top-view of the demonstration path to the toilet is shown in Figure 7. The differential flatness paradigm was used to plan the entire trajectory to the goal point within the demonstration scenario shown in Figure 7. In the simulation, three via points were chosen as intermediate points between the start and the goal. In the implementation, it is considered that the HLPR Chair arrives at a via point when it reaches within a radius ε around it. A representative simulation is shown in Figure 8. In the actual experiments, we expect to localize the states of the vehicle and the obstacles through on-board sensors. Via points will then be selected based on these sensed data and trajectories will be developed based on the paradigm of differential flatness, which is well suited for near real-time implementations.

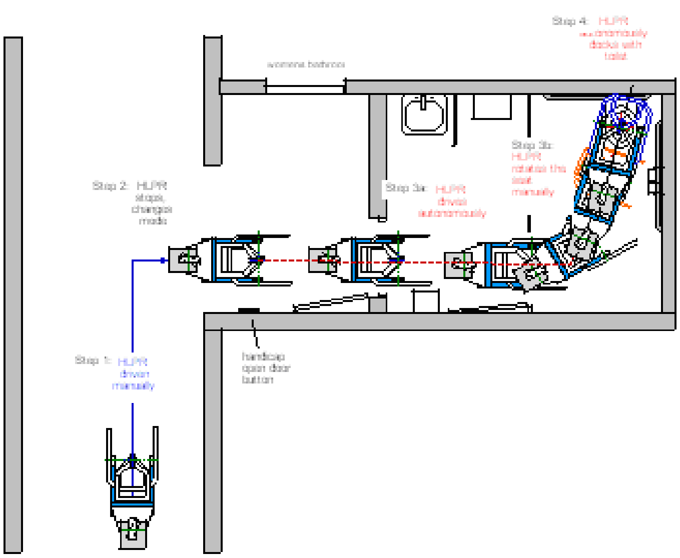

Figure 7. A graphic top-view of a demonstration path to the toilet

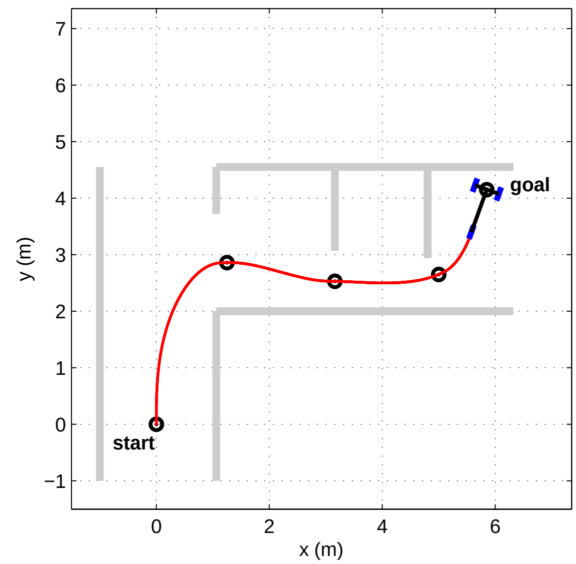

Figure 8. A simulation of a trajectory to the toilet using the differential flatness paradigm

5 Conclusions

The HLPR Chair is a novel mobility-assist patient lift system with an autonomous capability. This system shows promise for moving wheelchair dependents, the elderly, and others requiring personal mobility and lift access into the work force. We believe that this system can reduce injuries in workers who take care of wheelchair dependents and will help to mitigate the burden placed on healthcare industry due to aging population. The system prototype shows the underlying concepts behind a patient lift and mobility system through arelatively inexpensive design. The powerful method of differential flatness will provide the near real-time navigation and control methodology that is required for autonomous navigation of the system integrating on-line sensors to localize the vehicle and the environment around it.

6 References

[1] Pollack, Martha, 'Intelligent Technology for Adaptive Aging, Presentation, AAAI-04 American Association for Artificial Intelligence Conference Keynote Address, 2004

[2] L.H.V. van der Woude , M.T.E. Hopman and C.H. van Kemenade, 'Biomedical Aspects of Manual Wheelchair Propulsion: The State of the Art II,' Volume 5, Assistive Technology Research Series, 1999, 392 pp., hardcover

[3] Thrun, Sebastian, Visit to Stanford University to discuss healthcare mobility devices, August 2006.

[4] Marras, William, 'Lifting Patients Poses High Risk for Back Injuries,' Ohio State University,

http://researchnews.osu.edu/archive/resthome.htm. 1999.

[5] Blevins, Healthcare Statistics: Blevins Medical, Inc., http://www.patientlift.net/282164.html. 2006

[6]U.S. Bureau of Labor Statistics, from Blevins website: http://www.patientlift.net/282164.html, 1994.

[7] John Henshaw, http://www.osha.gov/SLTC/ nursinghome/solutions.html, Occupational Safety and Health Administration, 2005

[8] Wasatch Digital iQ, 'InTouch Health's Remote Presence Robot Used by Healthcare Experts, Santa Barbara, CA and Salt Lake City –(Business Wire)–June 16, 2003.

[9] Bostelman, Roger; Albus, James, 'Survey of Patient Mobility and Lift Technologies Toward Advancements and Standards', NISTIR No. 7384, 2006.

[10] NIST Intelligent Control of Mobility Systems Program website: http://www.isd.mel.nist.gov/

[11] Kuno, Y., Murashima, T., Shimada, N., Shirai, Y., 'Intelligent Wheelchair Remotely Controlled by Interactive Gestures,' International Conference on Pattern Recognition, vol. 04, no. 4, p. 4672, 2000.

[12] Patel, S., Jung, S-H., Ostrowski, J., Rao, R., Taylor, C., 'Sensor based door navigation for a nonholonomic vehicle,' GRASP Laboratory, University of Pennsylvania, Proceedings of the 2002 IEEE International Conference on Robotics and Automation, Washington, DC, May 2002.

[13] Song W.-K.; Lee H.; Bien Z., 'KAIST - KARES: Intelligent wheelchair-mounted robotic arm system using vision and force sensor,' Robotics and Autonomous Systems, vol. 28, no. 1, pp. 83-94(12), 31, Publisher: Elsevier Science, July 1999.

[14] Yanco, H., Hazel, A., Peacock, A., Smith, S. and Wintermute, H. 'Initial Report on Wheelesley: A Robotic Wheelchair System,' Department of Computer Science, Wellesley College, 1995

[15] Bostelman, R., Albus, J., 'HLPR Chair A Service Robot for the Healthcare Industry,' 3rd International Workshop on Advances in Service Robotics, Vienna, Austria, July 7, 2006

[16] Dobkin, B., Apple, D., Barbeau, H., Basso, M., Behrman, A., Deforge, D., Weight-supported treadmill vs overground training for walking after acute incomplete SCI, Neurology, vol. 66, no. 4, 2006, pp 484-93.

[17] Albus, James; Bostelman, Roger; Hong, Tsai; Chang, Tommy; Shackleford, Will; Shneier, Michael; Integrating Learning into a Hierarchical Vehicle Control System, Integrated Computer-Aided Engineering Journal, 2006.

[18] Sira-Ramirez, Hebertt; Agrawal, Sunil K.; Differentially Flat Systems, Marcel Dekker (Control Engineering Series), Hardbound, ISBN 0-8247-5470-0, June 2004, 467 pages.

[19] M. Fliess, J. Levine, P. Martin, and P. Rouchon, 'Flatness and defect of non-linear systems: Introductory theory and examples', Int. J. of Control, Vol. 61, No. 6, pp. 1327-1361, 1995.

[20] B. dAndrea-Novel, G. Campion, and G. Bastin, 'Control of Nonholonomic Wheeled Mobile Robots by State Feedback Linearization', The Int. J. of Robotic Research, Vol. 14, No. 6, pp. 543-559, 1995.

[21] Y. Hao, B. Laxton, E. R. Benson, and S. K. Agrawal, 'Differential Flatness-Based Formation Following of a Simulated Autonomous Small Grain Harvesting System', Trans. of the Am. Soc. of Agric. Eng.(ASAE), Vol. 47, No. 3, pp. 933-941, 2004.

[22] Fossas, E., Franch, J., and Agrawal, S. K. 'Linearization by Prolongations of Two-input Driftless Systems,', Proc. IEEE Conf. on Decision and Control, pp. 3381-3385, 2000.